LAWRENCE
LIVERMORE
NATIONAL
LABORATORY

LLNL-TR-788954

MULTITAPER SPECTRAL ESTIMATION: An Alternative to the Welch Periodogram Approach

J. V. Candy

September 5, 2019

Disclaimer

This work performed under the auspices of the U.S. Department of Energy by Lawrence Livermore National Laboratory under Contract DE-AC52-07NA27344.

MULTITAPER SPECTRAL ESTIMATION: An Alternative to the Welch Average Periodogram Approach

J. V. Candy

Dynamic structural systems either operational or under test require complex spectral analysis in order to characterize their modal responses. In some applications constant vigilance in terms of analysis or potential failures demand an accurate methodology to estimate both modal frequencies as well as mode shapes. Typically, classical periodogram spectra are windowed and averaged applying the well-known Welch periodogram methodology (*WPM*) for spectral estimation [1]. In this report we discuss an alternative technique—the Multitaper Method (*MTM*) that can be applied to solve this challenging problem especially in the case of noisy, uncertain accelerometer measurements [2]. This approach is based on the development of a set of orthogonal tapers or windows enabling a superior statistical performance alleviating the need to section/overlap the measured data. Therefore, the *MTM* is capable of producing reliable and accurate spectral estimates enabling the extraction of the structural modal vibration frequencies.

1 INTRODUCTION

Dynamic structural systems operating in noisy environments create a challenging analysis and monitoring problem in order to estimate their signatures in real-time and predict potential anomalies that can lead to catastrophic failure. In order to estimate the condition of a structure from noisy vibration measurements, it is necessary to identify features that make it unique such as emitted resonant (modal) frequencies that offer a signature characterizing its condition. The monitoring of structural modes to estimate the condition of a device under investigation is essential, especially if it is a critical entity of an operational system. Many simple algorithms like the fast-Fourier transform coupled with spectral peak-picking offer a technique to extract modal frequencies of a structural object for both computational speed and accuracy [3]-[7]. Here we investigate a *classical* spectral estimation technique that enables an accurate extraction of modal frequencies from noisy uncertain measurements.

Spectral estimation is a necessary methodology to analyze the frequency content of noisy data sets. Many techniques have evolved starting with the classical Fourier transform methods based on the well-known Wiener-Khintchine relationship relating the covariance-to-spectral density as a transform pair culminating with more elegant model-based, parametric techniques that apply prior knowledge of the data to produce a high-resolution spectral estimate [8], [9]. Perhaps, a far less popular, but powerful methodology that has emerged is the Multitaper Method (*MTM*) developed by Thomson [10]. The *MTM* evolved from the need to reduce spectral leakage that creates smearing in the frequency domain along

with other undesirable properties such as local and broadband biases as well as uncertainty increasing the overall error variance [11]. *Windowing* or equivalently *tapering* methods in Fourier-based spectral estimation are well-known ([8],[9]) leading to improved statistical performance. The popular *correlation* or so-called *Blackman-Tukey* method [8] that Fourier transforms a windowed covariance satisfying the Wiener-Khintchine relationship directly was developed with the advent of the fast Fourier transform (*FFT*). Currently for long data records, the most popular approach is the Welch Periodogram Method (*WPM*) that is based on averaging normalized periodograms estimated from windowed, overlapped sections of data [1]. Here the usual trade-off between estimator *bias/variance* dominates the spectral design. The *MTM* falls into this class of spectral estimators with the underlying difference that its inherent windows are a set of orthogonal prolate spheroidal wave functions that lead to a unique set of decomposed "eigen-spectra" that are averaged to reduce error variance, similar to the *WPM*. It is this specific set of windows (tapers) that provide interesting statistical properties leading to vastly improved spectral estimates [10].

In this Sec. 2, we briefly discuss the fundamental background material to comprehend spectral estimation techniques. Classical spectral estimators are breifly discussed in Sec. 3 leading to the detailed development of the multitaper method along with its properties and extensions. In Sec. 4 a simple sinusoidal simulation is developed to demonstrate the performance of this *MTM* approach and compare its performance to that of *WPM* on both deterministic and noisy (0dB SNR) data. We summarize our results and conclusions in the final section.

2 BACKGROUND

We can apply a filter to a random signal, but since its output is still random, we must find a way to eliminate or reduce this randomness in order to employ the powerful techniques available from systems theory. In this section, we shall show that techniques from statistics combined with linear systems theory can be applied to extract the desired signal information and reject the disturbance or noise.

Techniques similar to linear deterministic systems theory hold when the random signal is transformed to its *covariance sequence* and its Fourier spectrum is transformed to its *power spectrum*. Once these transformations are accomplished, then the techniques of linear systems theory can be applied to obtain results similar to deterministic signal processing. In fact, we know that the covariance sequence and power spectrum are a discrete Fourier transform pair, analogous to a deterministic signal and its corresponding spectrum, that is, we have that

$$\text{Fourier Transform}: \qquad R(k) \longleftrightarrow S_{xx}(\Omega)$$

and as in the deterministic case, we can analyze the spectral content of a random signal by investigating its power spectrum.

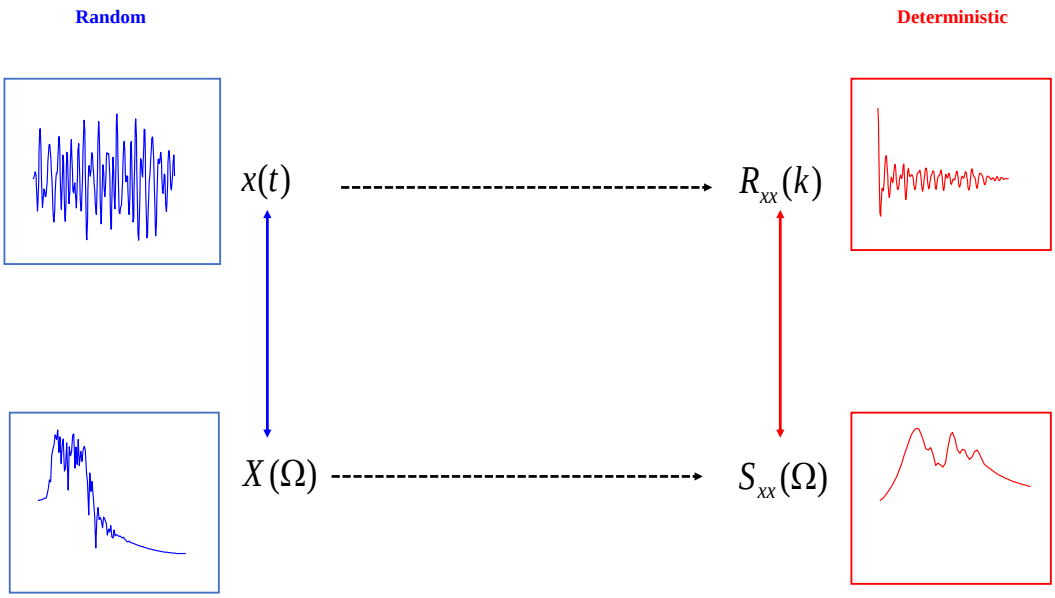

Figure 1: Random Signal Comparison: Random signal and spectrum and the deterministic covariance and power spectrum.

The *power spectral density* (*PSD*) function for a discrete random process is defined as:

$$S_{xx}(\Omega) = \lim_{N\to\infty} E\left\{\frac{X(\Omega)X^*(\Omega)}{2N+1}\right\} \tag{1}$$

where * is the complex conjugate. The expected value operation, $E\{.\}$, that can be thought of as "mitigating" the randomness. Similarly, the *covariance*[1] of the process is defined by:

$$R_{xx}(k) := E\left\{x(t)x(t+k)\right\} - E^2\{x(t)\} \tag{2}$$

In a sense these relations replace the random signals, but play the same role as their deterministic counterparts. These concepts are illustrated in Fig. 1 where we see the random signal and it random Fourier transform replaced by the deterministic covariance and its deterministic power spectrum.

Techniques of linear systems theory for random signals are valid, just as in the deterministic case where the covariance at the output of a system excited by a random signal $x(t)$, is given by the convolution relationship in the temporal or frequency domain as,

$$\text{Convolution}: \qquad R_{yy}(k) \;=\; h(t) * h(-t) * R_{xx}(k)$$

[1]It is also common to use the so-called *correlation* function, which is merely the mean-squared function and identical to the covariance function for a mean of zero.

$$\text{Multiplication}: \qquad S_{yy}(\Omega) \;=\; H(\Omega)H^*(\Omega)S_{xx}(\Omega) = |H(\Omega)|^2 S_{xx}(\Omega) \tag{3}$$

Analogously, the filtering operation is performed by an estimation filter, $\hat{H}_f$, designed to shape the output *PSD*, similar to the deterministic filtering operation

$$\text{Filtering}: \qquad S_{yy}(\Omega) = \mid \hat{H}_f(\Omega) \mid^2 S_{xx}(\Omega) \tag{4}$$

2.1 Spectral Representation of Random Signals

In many engineering problems before the design of processing algorithms can proceed, it is necessary to analyze the measured signal. Analogous to the deterministic case, the covariance function transforms the random signal and the power spectrum (transforms) its Fourier transform for analysis as illustrated in Fig. 1. In this section, we derive the relationship between the covariance function and power spectrum and show how they can be used to characterize fundamental random signals.[2].

First we begin by defining the power spectrum of a discrete random signal. Recall that the *discrete-time Fourier transform* (*DtFT*) pair is given by [13]

$$\begin{aligned} X(e^{j\Omega}) \;&:=\; DtFT[x(t)] = \sum_{t=-\infty}^{\infty} x(t)e^{-j\Omega t} \\ x(t) \;&=\; IDtFT[X(e^{j\Omega})] = \frac{1}{2\pi}\int_{2\pi} X(e^{j\Omega})e^{j\Omega t}d\Omega \end{aligned} \tag{5}$$

If $x(t)$ is random, then $X(e^{j\Omega})$ is *also* random because

$$x(t,\xi_i) \Longleftrightarrow X(e^{j\Omega},\xi_i) \quad \forall\; i$$

both are simply realizations of a random signal over the ensemble generated by i. Also, and more important, $X(e^{j\Omega})$ for stationary processes almost never exists because any non-zero realization $x(t,\xi_i)$ is not absolutely summable in the ordinary sense (these integrals can be modified (see [14] or [15] for details)).

Now let us develop the relationship between the *PSD* and its corresponding covariance. We have

$$S_{xx}(e^{j\Omega}) = \lim_{N\to\infty} \frac{1}{2N+1} E\left\{X_N(e^{j\Omega})X_N^*(e^{j\Omega})\right\} \tag{6}$$

Substituting for the *DtFT*, moving the expectation operation inside the summation and introducing a change of variable gives the relation

[2]We shall return to more mathematically precise notation for this development, that is, $X(\Omega) = X(e^{j\Omega})$

$$S_{xx}(e^{j\Omega}) = \sum_{k=-\infty}^{\infty} E_T\{R_{xx}(m+k,m)\}e^{-j\Omega k} \tag{7}$$

If we further assume that the process is wide-sense stationary, then $R_{xx}(m+k,m) \rightarrow R_{xx}(k)$ is no longer a function of time, but lag k and therefore,

$$S_{xx}(e^{j\Omega}) = \sum_{k=-\infty}^{\infty} R_{xx}(k)e^{-j\Omega k} \tag{8}$$

evolves as the well-known *Wiener-Khintchine* relation with the corresponding covariance given by *IDtFT*

$$R_{xx}(k) = \frac{1}{2\pi}\int_{2\pi} S_{xx}(e^{j\Omega})e^{j\Omega k}d\Omega \tag{9}$$

Recall that the *DtFT* is just the $\mathcal{Z}$-transform of $x(t)$ evaluated on the unit circle, that is,

$$S_{xx}(\Omega) = S_{xx}(z)|_{z=e^{j\Omega}}$$

and we obtain the equivalent pair in terms of the $\mathcal{Z}$-transform as

$$S_{xx}(z) = Z[R_{xx}(k)] = \sum_{k=-\infty}^{\infty} R_{xx}(k)z^{-k}$$

and

$$R_{xx}(k) = \frac{1}{2\pi j}\int S_{xx}(z)z^{k-1}dz \tag{10}$$

In practice, the auto-covariance and power spectrum find most application in the *analysis* of random signals yielding information about spectral content, periodicities, etc., while the cross-covariance and spectrum are used to estimate the properties of two distinct processes (e.g. input and output of a system) to follow. Before we discuss these estimators, it will be necessary to define some of the common terms embedded in spectral estimation.

Consider a finite duration realization defined by

$$x_N(t) := \begin{cases} x_N(t,\xi_i) & |t| \leq N < \infty \\ 0 & |t| > N \end{cases}$$

Note that $x_N(t)$ will be absolutely summable (N finite) if $x(t)$ has a finite mean-squared value and in fact $x_N(t)$ will also have finite energy, therefore, it will be Fourier transformable. The average power of $x_N(t)$ over the interval $(-N,N)$ is

$$\textit{Average power} = \frac{1}{2N+1}\sum_{t=-N}^{N} x^2(t) = \frac{1}{2N+1}\sum_{t=-\infty}^{\infty} x_N^2(t)$$

Table 1: Properties of Covariance and Spectral Functions.

	Covariance	Power Spectrum
1.	*Average Power*:	
	$R_{xx}(0) = E\{x^2(t)\}$	$R_{xx}(0) = \frac{1}{2\pi}\int_{2\pi} S_{xx}(z)z^{-1}dz$
2.	*Symmetry*:	
	$R_{xx}(k) = R_{xx}(-k)$ (even)	$S_{xx}(z) = S_{xx}(z^{-1})$ (even)
	$R_{xy}(k) = R_{yx}(-k)$	$S_{xy}(z) = S^*_{yx}(z)$
3.	*Maximum*:	
	$R_{xx}(0) \geq \lvert R_{xx}(k)\rvert$	$S_{xx}(e^{j\Omega}) \geq 0$
	$\frac{1}{2}R_{xx}(0) + \frac{1}{2}R_{yy}(0) \geq \lvert R_{xy}(k)\rvert$	
	$R_{xx}(0)R_{yy}(0) \geq \lvert R_{xy}(k)\rvert^2$	
4.	*Real*:	
		$S_{xx}(z) = E\{\lvert X(z)\rvert^2\}$ is real
		$S_{xy}(z) = E\{X(z)Y^*(z)\}$ is complex
5.	*Sum Decomposition*:	
		$S_{xx}(z) = S^+_{xx}(z) + S^-_{xx}(z) - R_{xx}(0)$

but by Parseval's theorem for discrete signals, we obtain the spectral representation for $x_N(t) \rightarrow X_N(\Omega)$

$$\sum_{t=-\infty}^{\infty} x_N^2(t) = \frac{1}{2\pi} \int_{2\pi} \mid X_N(e^{j\Omega}) \mid^2 d\Omega$$

where $|X_N(e^{j\Omega})|^2 = X_N(e^{j\Omega}) X_N^*(e^{j\Omega})$, * the conjugate and we have

$$Average\ power = \int_{2\pi} \left(\frac{|X_N(e^{j\Omega})|^2}{2N+1} \right) \frac{d\Omega}{2\pi}$$

The quantity in parentheses represents the average power per unit bandwidth and is the power spectral density of $x_N(t)$. Since x_N is a realization of a stochastic process, we must average over the ensemble of realizations

$$S_{x_N x_N}(e^{j\Omega}) = E \left\{ \frac{|X_N(e^{j\Omega})|^2}{2N+1} \right\}$$

but since $x_N \rightarrow x$ as $N \rightarrow \infty$ we obtain the *power spectral density* (*PSD*) of $x_N(t)$ as before

$$S_{xx}(e^{j\Omega}) = \lim_{N \rightarrow \infty} E \left\{ \frac{|X_N(e^{j\Omega})|^2}{2N+1} \right\}$$

With this in mind, we define the (raw) *periodogram* spectrum by

$$\hat{P}(\Omega) := \frac{1}{N} \Big| X(\Omega) \Big|^2 = \frac{1}{N} \Big| \sum_{t=0}^{N} x(t) e^{-j\Omega t} \Big|^2 \tag{11}$$

which is *poor* estimator asymptotically *unbiased* for large N, but with a very *large variance* that is quadratic, that is,

$$Bias\Big(\hat{P}(\Omega)\Big) = \hat{P}(\Omega) \qquad \text{and} \qquad Var\Big(\hat{P}(\Omega)\Big) = \hat{P}^2(\Omega) \tag{12}$$

Next we consider a more direct approach to estimate the *PSD*. An improved method of spectral estimation based on the *periodogram* defined by the Wiener-Khintchine relation and the *DFT*

$$P_{xx}(\Omega_m) := \frac{1}{N} |X(\Omega_m)|^2 = \frac{1}{N} \sum_{k=-(N-1)}^{N-1} R_{xx}(k) e^{-jk\Omega_m}$$

where the discrete frequency $\Omega_m = (\frac{2\pi}{2N+1} m$ and $\hat{R}_{xx}$ the a biased correlation estimator such that [9]

$$\hat{R}_{xx}(k) = \frac{1}{N} \sum_{t=0}^{N-1} x(t) x(t+k)$$

with *bias*

$$E\{P_{xx}(\Omega_m)\} = \frac{1}{N}\sum_{k=-(N-1)}^{N-1} E\{R_{xx}(k)\}e^{-jk\Omega_m} = \frac{1}{N}\sum_{k=-(N-1)}^{N-1}\left(1-\frac{|k|}{N}\right)R_{xx}(k)e^{-jk\Omega_m}$$

which is biased not just because of $\frac{|k|}{N}$, but also because of the finite limits on the summation. If we identify the term $(1-\frac{|k|}{N})$ as a triangular lag window function, $\mathcal{W}(k) = 1-\frac{|k|}{N}$, then

$$E\{P_{xx}(\Omega_m)\} = DFT[R_{xx}(k)\mathcal{W}(k)] = \mathcal{W}(\Omega_m) * S_{xx}(\Omega_m) \tag{13}$$

So we see that the expected value of the periodogram is the true spectrum $S_{xx}(\Omega_m)$ observed through the spectral window $\mathcal{W}(\Omega_m)$. Note that a rectangular data window results in a triangular correlation or Bartlett window or the so-called discrete *Dirichlet kernel* (squared) as

$$\mathcal{W}(\Omega_m) = \frac{1}{N}\left[\frac{\sin\left(\Omega_m\frac{N}{2}\right)}{\sin\left(\frac{\Omega_m}{2}\right)}\right]^2$$

for the spectral window.

Recall that most windows trade off main lobe width for side lobe height. For large N, the spectral window, $\mathcal{W}$ will have a narrow main lobe along with narrow side lobes. In this case, we see that

$$E\{P_{xx}(\Omega_m)\} \approx S_{xx}(\Omega_m)$$

and that the periodogram is asymptotically ($N \to \infty$) unbiased. In order for the periodogram estimate to be good, it must have a small variance as N increases. Unfortunately, $var\{P_{xx}(\Omega_m)\}$ is generally not small even for large N. For example, if x is a white Gaussian process, then it can be shown (see [9]) that

$$\lim_{N\to\infty} var\{P_{xx}(\Omega_m)\} = S_{xx}^2(\Omega_m)$$

that is, the variance of the periodogram approaches the square of the true spectrum at each m. In fact, in general, it can be shown that

$$var\{P_{xx}(\Omega_m)\} = S_{xx}^2(\Omega_m)\left[1+\left(\frac{\sin(N\Omega_m)}{N\sin(\Omega_m)}\right)^2\right]$$

which implies that as N increases, the variance is proportional to S_{xx}^2 as before and therefore P_{xx} is *not* consistent ($N\to\infty : Var \not\approx 0$). Similarly, it can be shown that the

$$cov\{P_{xx}(\Omega_m)P_{xx}(\Omega_j)\} \approx P_{xx}(\Omega_m)P_{xx}(\Omega_j)\left\{\left(\frac{\sin N/2(\Omega_m+\Omega_j)}{N\sin(\Omega_m+\Omega_j)/2}\right)^2 + \left(\frac{\sin N/2(\Omega_m-\Omega_j)}{N\sin(\Omega_m-\Omega_j)/2}\right)^2\right\}$$

Since this relation is evaluated at equally spaced frequency samples, we see that the samples are uncorrelated giving the periodogram a wildly fluctuating appearance and χ_2^2 distribution [9]. Since the samples of P_{xx} are uncorrelated, this suggests that one way of reducing the variance in P_{xx} is to individual periodograms, obtained by sectioning the original N point data record into K, L-point sections, that is,

$$\hat{S}_{xx}(\Omega_m) = \frac{1}{K}\sum_{i=1}^{K} \hat{P}_{xx}(\Omega_m, i)$$

where $\hat{P}_{xx}(\Omega_m, i)$ is the $i-th, L-point$ periodogram. If x is stationary, then

$$E\{\hat{S}_{xx}(\Omega_m)\} = \frac{1}{K}\sum_{i=1}^{K} E\{\hat{P}_{xx}(\Omega_m, i)\} = E\{\hat{P}_{xx}(\Omega_m, i)\} = S_{xx}(\Omega_m)$$

that is unbiased. If we introduce a spectral smoothing window as before, then

$$E\{\hat{S}_{xx}(\Omega_m)\} = \frac{1}{L} S_{xx}(\Omega_m) * \mathcal{W}(\Omega_m) \quad \text{where } L = \frac{N}{K}$$

which for impulse window functions gives

$$E\{\hat{S}_{xx}(\Omega_m)\} \propto \frac{K}{N} S_{xx}(\Omega_m)$$

Again assuming independence of the x, we have

$$var\{\hat{S}_{xx}(\Omega_m)\} = \frac{1}{K} var\{\hat{P}_{xx}(\Omega_m, i)\} \approx \frac{1}{K} S_{xx}^2(\Omega_m)\left[1 + \left(\frac{\sin K\Omega_m}{K \sin \Omega_m}\right)^2\right]$$

So we see that this estimate is consistent, since the variance approaches zero as the number of sections become infinite. We conclude that for the basic averaged periodogram estimator

$$var \propto \frac{1}{K} \quad \text{and} \quad bias \propto \frac{K}{N}$$

but that for K large, the variance becomes small, but the bias increases. Therefore for a *fixed* record length N as the number of periodograms increases, variance decreases, but the bias increases. This is the basic *tradeoff* between variance and bias (resolution) that can be used to determine a priori the required record length $N = LK$ for an acceptable variance. If we use a lag window to obtain a smoothed spectral estimate, then the variance can be approximated by

$$var\{\hat{S}_{xx}(\Omega_m)\} \approx \left(\frac{1}{N\triangle T} \sum_{k=-(K-1)}^{K-1} \mathcal{W}^2(k)\right) S_{xx}^2(\Omega_m)$$

assuming the window length is narrow relative to variations of $S_{xx}(\Omega_m)$, yet wide compared to the triangular lag window as discussed previously for the correlation estimate.

So we see that the properties of covariance and spectra not only can be used to analyze the information available in random signal data, but also to estimate various signal characteristics. In the next section we will investigate the properties of linear systems excited by random inputs and use the properties of covariance and spectra to analyze the results. Therefore, we can define random signals in terms of their covariances and spectral densities.

A purely random or *white noise* sequence, $e(t)$, is a sequence in which all the $e(t)$ are mutually independent, that is, knowing $e(t)$ in no way can be used to predict $e(t+1)$. A white sequence is called completely random or unpredictable or memoryless (no correlation). Sequences of this type have historically been called white because of their analogy to white light, which possesses all frequencies (constant power spectrum), that is, the power spectral density of white noise is

$$S_{ee}(\Omega) = R_{ee} \qquad \text{(constant)}$$

with the corresponding covariance is given by

$$R_{ee}(k) = R_{ee}\delta(k)$$

where R_{ee} is the variance of the noise.

In fact, the white noise characterization of *random* signals is analogous to the unit impulse representation of *deterministic* signals, that is,

$$R_{ee}\delta(k) \Longleftrightarrow A\delta(t)$$

and

$$S_{ee}(\Omega) = R_{ee} \Longleftrightarrow H(\Omega) = A$$

It is the random counterpart for random systems of the unit impulse excitation for the analysis of linear time invariant (*LTI*) systems.

Some properties of the discrete covariance function for stationary processes along with accompanying properties of the *PSD* are given (without proof see [13] for details) in Table 1 for reference.

It is important to recognize that these properties are essential to analyze the information available in a discrete random signal. For instance, if we are trying to determine phase information about a particular measured signal, we immediately recognize that it is lost in both the auto-covariance and corresponding output power spectrum.

2.2 Discrete Systems with Random Inputs

When random inputs are applied to linear systems, then covariance and power spectrum techniques must be applied transforming the signal and its Fourier spectrum in deterministic signal theory (see Fig. 1). In this section, we develop the relationship between systems and random signals. From linear systems theory, we have the convolution or equivalent frequency relations

$$y(t) = h(t) * x(t) = \sum_{k=0}^{\infty} h(k)x(t-k) \tag{14}$$

or taking discrete-time Fourier transforms, we obtain

$$Y(\Omega) = H(\Omega)X(\Omega) \tag{15}$$

If we assume that x is a random signal then as we have seen in the previous section, we must resort to spectral representations of random processes. Exciting a causal linear system with a zero-mean random signal, we obtain the output power spectrum

$$S_{yy}(\Omega) = E\{Y(\Omega)Y^*(\Omega)\} = E\left\{\Big(H(\Omega)X(\Omega)\Big)X^*(\Omega)H^*(\Omega)\right\} = |H(\Omega)|^2 S_{xx}(\Omega) \tag{16}$$

or equivalently

$$S_{yy}(\Omega) = E\left\{Y(\Omega)Y^*(\Omega)\right\} = E\left\{Y(\Omega)\Big(X^*(\Omega)H^*(\Omega)\Big)\right\} = S_{yx}(\Omega)H^*(\Omega) \tag{17}$$

Perhaps one of the most important properties that has led to a variety of impulse response identification techniques is

$$S_{yx}(\Omega) = E\left\{Y(\Omega)X^*(\Omega)\right\} = E\left\{H(\Omega)\Big(X(\Omega)X^*(\Omega)\Big)\right\} = H(\Omega)S_{xx}(\Omega) \tag{18}$$

solving for H provides the *Wiener solution* in the frequency domain.
Similar results can be obtained for auto and cross-covariances and corresponding spectra. We summarize these linear system relations in Table 2.

3 SPECTRAL ESTIMATION

Spectral estimation techniques have been developed and improved over the years with one major task in mind—the analysis of random data. Based on the previous discussion in this chapter, a majority of the initial effort was focused on applying the Wiener-Khintchine theorem and transform theory, while modern parametric techniques evolved primarily from the "speech" community [16], [17]. In this section, we discuss popular classical (nonparametric) methods that are viable when *long* data records are available. We make no attempt to provide detailed derivations of the algorithms that are available in other texts [13], [16], [18], [19], but just follow a brief outline of the approach and present the final results.

3.1 Classical (Nonparametric) Spectral Estimation

With the initial application of Fourier analysis techniques to raw sun-spot data over 200 years ago, the seeds of spectral estimation were sown by Schuster [20]. Fourier analysis for random signals evolved rapidly after the discovery of the Wiener-Khintchine theorem

Table 2: Linear System with Random Inputs: Covariance/Spectrum Relationships.

Covariance	Spectrum
$R_{yy}(k) = h(k) * h(-k) * R_{xx}(k)$	$S_{yy}(z) = H(z)H(z^{-1})S_{xx}(z)$
$R_{yy}(k) = h(k) * R_{xy}(k)$	$S_{yy}(z) = H(z)S_{xy}(z)$
$R_{yx}(k) = h(k) * R_{xx}(k)$	$S_{yx}(z) = H(z)S_{xx}(z)$

where

$R_{yy}(k) = \frac{1}{2\pi j} \oint S_{yy}(z) z^{k-1} dz$	$S_{yy}(z) = \sum_{k=-\infty}^{\infty} R_{yy}(k) z^{-k}$
$R_{xy}(k) = \frac{1}{2\pi j} \oint S_{xy}(z) z^{k-1} dz$	$S_{xy}(z) = \sum_{k=-\infty}^{\infty} R_{xy}(k) z^{-k}$

relating the covariance and power spectrum. Finally with the evolution of the fast Fourier transform (see Cooley [8]) and digital computers, all of the essential ingredients were present to establish the classical approach to nonparametric spectral estimation.

Classical spectral estimators typically fall into two categories: direct and indirect. The direct methods operate directly on the raw data to transform it to the frequency domain and produce the estimate. Indirect methods, first estimate the covariance sequence and then transform to the frequency domain–an application of the Wiener-Khintchine theorem. We develop two basic nonparametric spectral estimation techniques: the correlation method (indirect) and the periodogram method (direct).

3.1.1 Correlation or Blackman-Tukey Method (BTM))

The *correlation method* or sometimes called the Blackman-Tukey method (BTM) is simply an implementation of the Wiener-Khintchine theorem: the covariance is obtained using a sample covariance estimator and then the *PSD* is estimated by calculating the *discrete Fourier transform* (DFT). The DFT transform pair is defined by

$$X(\Omega_m) \;:=\; DFT\Big[x(t)\Big] = \sum_{t=0}^{M-1} x(t) e^{-j\Omega_m t}$$

$$x(t) \quad = \quad IDtFT\Big[X(\Omega_m)\Big] = \frac{1}{M}\sum_{t=0}^{M-1} X(\Omega_m)e^{j\Omega_m t} \tag{19}$$

for $\Omega_m = \frac{2\pi}{M}m$ where it can be thought of as the *DtFT* with $\Omega \to \Omega_m$, that is, the *DtFT* sampled uniformly around the unit circle [13].

Therefore, we have that

$$\hat{S}_{xx}(\Omega_m) \quad = \quad \text{DFT}\Big[\hat{R}_{xx}(k)\Big]$$

$$\hat{R}_{xx}(k) \quad = \quad \text{IDFT}\Big[\hat{S}_{xx}(\Omega_m)\Big]$$

This technique tends to produce a noisy spectral estimate; however, a smoothed estimate can be obtained by multiplying R_{xx} by a *window function*, $\mathcal{W}$ usually called a *lag window*. The window primarily reduces spectral leakage and therefore improves the estimate. It is also interesting to note that a sample covariance estimator does not guarantee the positivity of the *PSD* (auto) when estimated directly from the Wiener-Khintchine theorem [13]. However, if the estimator is implemented directly in the Fourier domain, then it will preserve this property, since it is the *square* of the Fourier spectrum.

We summarize the *correlation method* (Blackman-Tukey) of spectral estimation by:[3]

Correlation (Blackman-Tukey) Method (*BTM*) Spectral Estimation:

1. *Calculate* the *DFT* of $x(t)$, that is, $X(\Omega_m)$
2. *Multiply* $X(\Omega_m)$ by its conjugate to obtain, $X(\Omega_m)X^*(\Omega_m)$
3. *Estimate* the covariance from the *IDFT*, $\hat{R}_{xx}(k) = IDFT\Big[|X(\Omega_m)|^2\Big]$
4. *Multiply* the covariance by the lag window $\mathcal{W}(k)$, and
5. *Estimate* the *PSD* from the *DFT* of the windowed covariance, $\hat{S}_{xx}(\Omega_m) = DFT\Big[\hat{R}_{xx}(k)\mathcal{W}(k)\Big]$

These correlation spectral estimates are statistically improved by using a lag or equivalently spectral window.[4] With practical window selection and long data records, the correlation method can be effectively utilized to estimate the *PSD* (see [13] for more details).

[3]Note also if we replace X^* by Y^* we can estimate the cross correlation $\hat{R}_{xy}(k)$ and corresponding cross spectrum $\hat{S}_{xy}(\Omega_m)$ using this method.

[4]The window function is called a *lag window* in the time or lag domain $\mathcal{W}(k)$ and a *spectral window* in the frequency domain $\mathcal{W}(\Omega_m)$ with its maximum at the origin to match that property of the autocorrelation function; therefore, it is sometimes called a "half" window.

3.1.2 Welch Average Periodogram Method (*WPM*)

Next we consider a more direct approach to estimate the *PSD*. We introduce the concept of a periodogram estimator with statistical properties equivalent to the correlation method, then we show how to improve these estimates by statistical averaging and window smoothing leading to *Welch's method* of spectral estimation, that is, the Welch Periodogram Method (*WPM*) [1]. The periodogram was devised by statisticians to detect periodicities in noisy data records [20]. The improved method of spectral estimation based on the so-called *periodogram* defined by

$$P_{xx}(\Omega_m) := \frac{1}{N}\left(X(\Omega_m)\ X^*(\Omega_m)\right) = \frac{1}{N}\Big|X(\Omega_m)\Big|^2$$

The samples of P_{xx} are uncorrelated, suggesting that one way of reducing the variance in P_{xx} is to *average* individual periodograms obtained by *sectioning* the original N point data record into K, L-point sections, that is,

$$\hat{S}_{xx}(\Omega_m) = \frac{1}{K}\sum_{i=1}^{K}\hat{P}_{xx}(\Omega_m, i)$$

where $\hat{P}_{xx}(\Omega_m, i)$ is the i-th, L-point periodogram. If x is stationary, then it can be shown that this estimate is consistent, since the variance approaches zero as the number of sections become infinite [13]. For the periodogram estimator, we have

$$var \propto \frac{1}{K} \quad \text{and} \quad bias \propto \frac{K}{N}$$

So we see that for K large, the variance is inversely proportional to K, while the bias is directly proportional. Therefore for a *fixed* record length N as the number of periodograms increases, variance decreases, but the bias increases. This is the basic tradeoff between variance and resolution (bias) which can be used to determine a priori the required record length $N = LK$ for an acceptable variance. A *full* window, $\mathcal{W}(t)$, can also be applied to obtain a smoothed spectral estimate.

Welch [1] introduced a modification of the original procedure. The data is sectioned into K records of length L; however, the window is applied directly to the segmented records *before* periodogram computation. The modified periodograms are then

$$\hat{P}(\Omega_m, i) = \frac{1}{U}\Big|DFT\Big[x_i(t)\mathcal{W}(t)\Big]\Big|^2 \quad i = 1, \ldots, K$$

where

$$U = \frac{1}{L}\sum_{t=0}^{L-1}\mathcal{W}^2(t)$$

and

$$\hat{S}_{xx}(\Omega_m) = \frac{1}{K}\sum_{i=1}^{K}\hat{P}(\Omega_m, i)$$

We summarize the *average periodogram method* (Welch's procedure) by:

Average Periodogram (Welch) Method (*WPM*) Spectral Estimation:

1. *Section* the data, $\{x(t)\}$, $t = 1, \ldots, N$ into K sections each of length L, where $K = \frac{N}{L}$, that is,

$$x_i(t) = x(t + L(i-1)), \quad i = 1, \ldots, K, \quad t = 0, \ldots, L-1$$

2. *Window* the data to obtain, $x_i(t) \times \mathcal{W}_i(t)$

3. *Estimate* K periodograms using the *DFT* as

$$\hat{P}(\Omega_m, i) = \frac{1}{U} \left| DFT\Big[x_i(t)\mathcal{W}(t)\Big] \right|^2 \quad i = 1, \ldots, K$$

with $U = \frac{1}{L} \sum_{t=0}^{L-1} \mathcal{W}^2(t)$

4. *Estimate* the average spectrum using

$$\hat{S}_{xx}(\Omega_m) = \frac{1}{K} \sum_{i=1}^{K} \hat{P}(\Omega_m, i)$$

with $\text{var}\{\hat{S}_{xx}(\Omega_m)\} \propto \frac{1}{K}$ and $\text{bias}\{\hat{S}_{xx}(\Omega_m)\} \propto \frac{K}{N}$ adjusted for particular windows.

3.2 Multitaper Method (*MTM*)

There are two primary performance metrics of high interest in a spectral estimators: bias and variance. Bias can be decomposed into two types: local and broadband. *Local bias* evolves from the underlying bandwidth of the main lobe of a spectral window (intentional or not) employed during the processing, while *broadband bias* is a direct function of its side lobes. Detrimental effects are a result of both either smearing frequency peaks (local bias) or creating bogus peaks in the estimate (broadband bias). Spectral estimators are designed to be "asymptotically unbiased" ($N \to \infty : bias \to 0$) and "asymptotically consistent" as well as ($N \to \infty : var \to 0$). Spectral uncertainties evolve from the leakage effects created by high side lobes and can be mitigated by averaging periodograms as in *WPM*.

With these metrics in mind, *local bias* can be decreased by decreasing the spectral window main lobe bandwidth making it narrower increasing frequency resolution leading to an asymptotically unbiased estimate. *Broadband bias* evolving from spectral leakage created by the underlying side lobes leaks the broad spectral components into the estimate at a

given frequency. Knowledge of these window-based detriments lead to an effective method to design spectral estimators, since

$$S_{xx}(\Omega) = \underbrace{|\mathcal{W}(\Omega)}_{Spectral\ Window} \quad * \quad X(\Omega)|^2 \tag{20}$$

Therefore, if $\mathcal{W}(\Omega)$ is designed with small side lobes, then leakage is minimized reducing broadband bias, but of course the tradeoff is that decreased side lobes lead to *wider* main lobe bandwidth decreasing *spectral resolution*.

The Multitaper Method (*MTM*) reduces bias by obtaining statistically independent estimates that can effectively be averaged to reduce uncertainty much like the Welch *WPM*. Each window of *MTM* is pairwise *orthogonal* to all other windows providing the statistically independent set of spectral estimates that are averaged (weighted) to provide the final spectrum. The orthogonal windows are *Slepian* discrete prolate spheroidal sequences (*DPSS*) that possess the required properties such as minimizing spectral leakage while concentrating the power in tight bands [12].

Recall that frequency resolution is specified by the number of samples, N, and the corresponding sampling interval $\triangle t$ determined by the highest frequency supported by the data, that is, the sampling frequency $f_s = \frac{1}{\triangle t}$ with corresponding Nyquist frequency, f_{NYQ}. Therefore, the *frequency resolution*, $\triangle f$ is

$$\triangle f := \frac{f_s}{N} = \frac{1}{N \triangle t} \qquad \text{and} \qquad f_{NYQ} = \frac{f_s}{2} \tag{21}$$

yielding the minimal frequency band that distinct sinusoids can be resolved [11].

MTM estimation, in its simplest form, is given by

$$\hat{S}_{MTM}(\Omega) = \frac{1}{K} \sum_{k=0}^{K-1} \hat{S}_{MTM}(\Omega, k) \tag{22}$$

and

$$\hat{S}_{MTM}(\Omega, k) = \frac{\triangle t}{K} \sum_{k=0}^{K-1} = \Big| \underbrace{\mathcal{W}_k(t)}_{DPSS} x(t) e^{-j\Omega t} \Big|^2 \tag{23}$$

with $\mathcal{W}_k(t)$ the k-th discrete prolate spheroidal sequence (*DPSS*) of length N or window associated with the corresponding eigen-spectrum $\hat{S}_{MTM}(\Omega, k)$ [10], [11], [12]
and the *spectral* window

$$\mathcal{W}_k(\Omega) = \triangle t \sum_{t=0}^{N-1} \mathcal{W}_k(t) e^{-j\Omega t} \tag{24}$$

such that the expectation is given by

$$\hat{\bar{S}}_{MTM}(\Omega) = E\Big\{\hat{S}_{MTM}(\Omega)\Big\} = \frac{1}{K}\int_{-f_{NYQ}}^{f_{NYQ}} \overline{\mathcal{W}}_k(\Omega - \Omega')\hat{S}_{MTM}(\Omega')d\Omega' \tag{25}$$

for

$$\overline{\mathcal{W}}_k(\Omega) = \frac{1}{K}\sum_{k=0}^{K-1} \mathcal{W}_k(\Omega)$$

For *MTM*, the windows are the orthogonal set of *DPSS* $\{\mathcal{W}_k(t)\}, k = 0, 1, \cdots, K-1; t = 0, 1, \cdots, N-1$ that are solutions of the so-called concentration problem.[5] Here lies the *key* to the *MTM* — design of spectral windows that solve the concentration problem. More specifically, we define

Among ALL window sequences $\{\mathcal{W}_k\}$ for a given duration $N\triangle t$ and pre-specified bandwidth $[-f_{BW}, f_{BW}]$, FIND the sequence that maximizes the spectral concentration within this band or equivalently obtain the optimal sequence that minimizes the side lobe energy *outside* the band.

That is, find a sequence such that the *spectral concentration* defined by $\lambda(N\triangle t, f_{BW})$ on the interval $[-f_{BW}, f_{BW}]$ is maximum where

$$\lambda(N\triangle t, f_{BW}) := \frac{\int_{-f_{BW}}^{f_{BW}} |\mathcal{W}(\Omega)|^2 d\Omega}{\int_{-f_{NYQ}}^{f_{NYQ}} |\mathcal{W}(\Omega)|^2 d\Omega} \tag{26}$$

then FIND $\{\mathcal{W}_k(t)\}, k = 0, 1, \cdots, K-1; t = 0, 1, \cdots, N-1$ such that $\lambda(N\triangle t, f_{BW})$ is a maximum.

The solution to this constrained optimization problem is available in [10]-[12] and becomes an eigenvalue problem defined by:

$$\sum_{t'=0}^{N-1} \frac{\sin 2\pi f_{BW}(t-t')}{\pi(t-t')} \times \mathcal{W}(t') = \lambda(N\triangle t, f_{BW}) \times \mathcal{W}(t); \qquad t = 0, 1, \cdots, N-1$$

or expanding we obtain a vector-matrix form as

$$\mathcal{D}(f_{BW}) \times \underline{\mathcal{W}}(t') = \underbrace{\lambda(N\triangle t, f_{BW})}_{eigenvalues} \times \underbrace{\underline{\mathcal{W}}(t)}_{eigenvectors} \tag{27}$$

where the matrix components are$\mathcal{D}_{t,t'} = \frac{\sin 2\pi f_{BW}(t-t')}{\pi(t-t')} \in \mathcal{R}^{N\times K}$.

Since this matrix $\mathcal{D}$ is positive definite, then the largest eigenvalue corresponds to the largest spectral concentration and therefore the corresponding eigenvector sequence, $\underline{\mathcal{W}}_0(t)$

[5]The spectral concentration problem consists of finding a finite length window sequence whose spectrum is most localized in a given frequency interval specified by $\pm f_{BW}$.

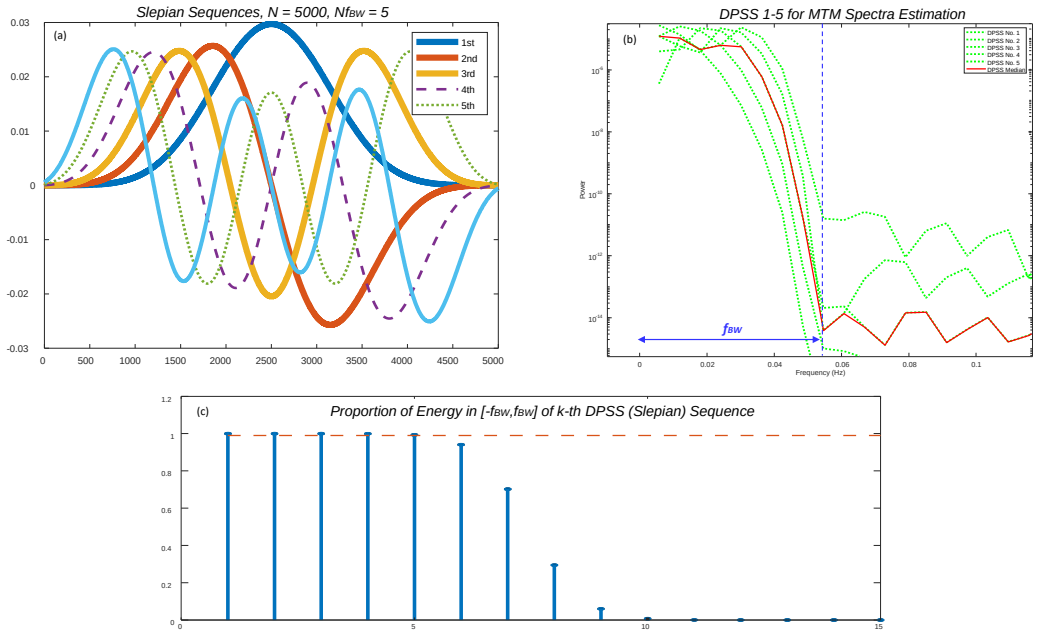

Figure 2: Discrete Prolate Spheroidal (Slepian) Sequences fo 8-mode, 3-channel structure. (a) DPSS. (b) DPSS spectra with f_{BW} bandwidth annotated. (c) Eigenvalues associated with each DPSS (5-dominant).

is termed the 0-th order *DPSS* (Slepian). The number of dominant eigenvalues of $\mathcal{D}$ are all close to unity and correspond to

$$\mathcal{S} := 2f_{BW} \times N\triangle t \qquad \text{[Shannon Number]} \tag{28}$$

with $\mathcal{S}$ defined as the *Shannon number* [11] with $\lambda_0 > \lambda_1, \cdots, \lambda_{K-1}$ where the $K-th$-order window offers the best side lobe suppression. In fact, the first $\mathcal{S}-1$ eigenvalues are close to unity indicating relatively *low* side lobe energy (leakage). We illustrate the calculation of the *DPSS*-windows in Fig. 2a where the first 5 functions are shown along with their corresponding spectra and functional bandwidth in (b). An application to a synthesized 8-mode mechanical system developed in Sec. 4 demonstrates the corresponding *DPSS*-eigenvalues in descending order in Fig. 2c. By imposing a unity threshold it is clear that the "optimal" *number* of *DPSS*s or equivalently *order* is 5, since their values are either at or above 1. This represents a convenient method for selection.

In the *MTM*, the length N-*DPSS* windows of orders $k = 0, 1, \cdots, (K-1)$ are usually applied in practice with $K \leq \mathcal{S} - 1$. *Fixed* N and f_{BW}, then lead to smaller values of K generally reduce leakage with larger values reducing variance. *Leakage* can be approximated by

$$\mathcal{L} = \frac{1}{K}\sum_{k=0}^{K-1}(1-\lambda_k(N\triangle t, f_{BW})) \qquad \text{[Leakage]} \tag{29}$$

and the corresponding *variance* is inversely proportional to the number of windows employed

$$var = \frac{1}{K} \qquad \text{[Variance]} \tag{30}$$

with frequency *resolution* specified by the design bandwidth, that is,

$$res = \triangle f = f_{BW} \qquad \text{[Resolution]} \tag{31}$$

Also, the *time-bandwidth* product is given by

$$\mathcal{T}_{BW} := \frac{\mathcal{S}}{2} := f_{BW} \times N\triangle t \tag{32}$$

It is this expression coupled with the number of windows that define the variance of *MTM* estimates. Choosing $\mathcal{T}_{BW}$ and K provide a tradeoff of spectral resolution, bias and variance. Bias is primarily controlled by the largest eigenvalue, $\lambda_0(N\triangle t, f_{BW})$ since

$$\lambda_0(N\triangle t, f_{BW}) \approx 1 - 4\pi\sqrt{\mathcal{T}_{BW}}e^{-2\pi\mathcal{T}_{BW}} \qquad \text{[Total Side Lobe Energy]} \tag{33}$$

the leakage outside $[-f_{BW}, f_{BW}]$ that decreases rapidly with increasing $\mathcal{T}_{BW}$ [21]-[24]. We summarize these properties below in Table 3.

Table 3.0 MTM LEAKAGE (Window) Properties [23]

MTM DPSS-Window (Slepian) Leakage Properties		
Time-Bandwidth ($\mathcal{T}_{BW}$)	**Asymptotic Leakage** ($1-\lambda_0$)	**Leakage** (dB)
4	3.05×10^{-10}	-95
6	1.31×10^{-15}	-149
8	5.26×10^{-21}	-203
10	2.05×10^{-26}	-257

So we see that it is in fact the optimal window design employing the *DPSS*s that enable the solution to the spectral concentration problem.

The *MTM* can be summarized as:

Multitaper Method (*MTM*) Spectral Estimation:

1. *Select* the frequency *resolution*: $f_{BW} < f_{NYQ}$ $Res = 2 \times f_{BW}$;
2. *Calculate* the time-bandwidth product (Shannon number): $\mathcal{S} = 2f_{BW} \times N\triangle t$;

3. *Calculate* the *number* of *DPSS*-functions (eigenvectors): $K \leq \mathcal{S} - 1$;

4. *Calculate* the *DPSS*-weights: $\mathcal{W}_k(t), k = 0, 1, \cdots, (K-1); t = 0, 1, \cdots, (N-1)$;

5. *Calculate* the individual eigen-spectra: $\hat{S}_{MTM}(\Omega, k) = \sum_{t=0}^{N-1} \mathcal{W}_k(t) x(t) e^{-j\Omega t}$;

6. *Estimate* the final *MTM* spectrum (averaging): $\hat{S}_{MTM}(\Omega) = \sum_{k=0}^{K-1} \hat{S}_{MTM}(\Omega, k)$;

Next we investigate extensions of the *MTM* spectral estimator using these Slepian sequences.

3.3 MTM Extensions

3.3.1 Eigenvalue Weighting

A reasonable *unbiased MTM* spectral estimate (*eigenvalue weighting method*) can be scaled by the associated eigenvalues such that

$$\hat{S}_{MTM}(\Omega) = \frac{\sum_{k=1}^{K-1} \lambda_k(N\triangle t, f_{BW}) \times |X_k(\Omega)|^2}{\sum_{k=1}^{K-1} \lambda_k(N\triangle t, f_{BW})} \tag{34}$$

the denominator ensures an unbiased estimate, while the individual eigenvalues (< 1) decrease the weighting of the larger spectra in the final estimate, since $\lambda_0 > \lambda_1 > \cdots > \lambda_K < 1$. That is, as the number of windows increase ($K \uparrow; \lambda \downarrow$), the corresponding eignenvalues decrease, mitigating more spectral leakage.

3.3.2 Adaptive Weighting

Another extension to the *MTM* proposed by Thomson is the *adaptive MTM* where a set of adaptive weights $\{\alpha_k(\Omega)\}$ are employed to downweight the higher order spectra using an iterative approach [11]. Here a weighted average of the eigen-spectra from individual *DPSS*s is performed leading to an iterative technique that adapts (adjusts) the weights for each band to provide a balance between broadband bias ($\mathcal{L}_k$) and the variance of the estimates. The following set of relations provide the iterations (over i):

$$\begin{aligned} \hat{S}_{MTM}(\Omega, i+1) &= \frac{\sum_{k=0}^{K-1} |\alpha_k(\Omega, i)|^2 \times \hat{S}_{MTM}(\Omega, k; i)}{\sum_{k=0}^{K-1} |\alpha_k(\Omega, i)|^2} \\ \alpha_k(\Omega, i) &= \frac{\sqrt{\lambda_k(N\triangle t, f_{BW})} \times S(\Omega, i)}{\lambda_k(N\triangle t, f_{BW}) S(\Omega, i) + \mathcal{L}_k} \end{aligned} \tag{35}$$

where $S(\Omega, 0)$ is the initial estimate of the power spectrum and $\mathcal{L}_k$ is the leakage that the k-th *DPSS* bank has at frequency Ω. The technique iterates over i converging to the desired solution completing the spectral estimation.

We summarize the major *properties* of the Multitaper Method (*MTM*):

- *Bias* is *local* characterized by the window main lobe width (resolution) and *broadband* characterized by the side lobes (leakage);
- *Local Bias* is *small* if the spectral window for $\hat{S}_{MTM}(\Omega)$ closely approximates $\frac{1}{2\times f_{BW}}$;
- *Broadband Bias* is *bounded* $(1 - \frac{1}{K}\sum_{k=0}^{K-1}\lambda_k(N\triangle t, f_{BW}))$ for K *DPSS*-windows;
- *Variance* is controlled by the *number* of *DPSS*-windows given by $var \approx \frac{1}{K}$;
- *Resolution* is specified (a-priori) by *twice* the design *bandwidth* of $2 \times f_{BW}$;
- *Mean-Squared Error* is *negligible*, if $k \leq \mathcal{S} - 1$ and $\{\lambda_k)(N\triangle t, f_{BW}) \approx 1$;
- *MTM* is a *direct method* of spectral estimation; and
- *MTM* can be applied to problems with *missing* or *irregularly-spaced* data sets.

This completes the discussion of the classical or nonparametric methods of spectral estimation. Even though they are considered classical techniques with limited resolution capability, they still can provide reasonable analytical information, if we have "long" data records with good signal levels. Next we consider an example that demonstrates this approach.

4 SPECTRAL ESTIMATION OF SIMULATED VIBRATION RESPONSE

In this section we study the application of *MTM* to estimate modal frequencies of a vibrating structure represented by a *LTI*, *MIMO*, mass-spring-damper mechanical system consisting of 8-modes or 16-states (see [26] for details) measured by 3-output accelerometers. The structure is excited by a random input. Structurally, the system mass ($\mathcal{M}$) is characterized by an identity matrix while the coupled spring constants in (N/m) are given by the tri-diagonal matrix

$$\mathcal{K} = \begin{bmatrix} 2400 & -1600 & 0 & 0 & 0 & 0 & 0 & 0 \\ -1600 & 4000 & -2400 & 0 & 0 & 0 & 0 & 0 \\ 0 & -2400 & 5600 & -3200 & 0 & 0 & 0 & 0 \\ 0 & 0 & -3200 & 7200 & -4000 & 0 & 0 & 0 \\ 0 & 0 & 0 & -4000 & 8800 & -4800 & 0 & 0 \\ 0 & 0 & 0 & 0 & -4800 & 10400 & -5600 & 0 \\ 0 & 0 & 0 & 0 & 0 & -5600 & 12000 & -6400 \\ 0 & 0 & 0 & 0 & 0 & 0 & -6400 & 13600 \end{bmatrix}$$

the damping matrix is constructed using the relation (Raleigh damping)

$$\mathcal{C}_d = 0.680\mathcal{M} + 1.743 \times 10^{-4}\mathcal{K} \quad \left(\frac{N\ s}{m}\right)$$

The measurement system consisted of three (3) accelerometers placed to measure the modes at the 1, 4 and 8 locations on the structure. The accelerometer data is acquired and digitized at a sampling frequency of $50Hz$ ($\triangle t = 0.02sec$). The input signal from a randomly excited stinger rod is applied at a specified spatial location such that

$$\mathcal{M}\ddot{\mathbf{d}}(t) + \mathcal{C}_d\dot{\mathbf{d}}(t) + \mathcal{K}\mathbf{d}(t) = \mathcal{B}_p\mathbf{p}(t)$$

Three accelerometer outputs of the synthesized vibrating structure was recorded for 200 *sec* with the vibrational responses shown in Fig. 3 along with their corresponding power spectra where we see a persistently excited system ideal for spectral estimation. The set of "true" modal frequencies corresponding to the spectral peaks are:

$$f_{TRUE} = \{2.94, 5.87, 8.60, 11.19, 13.78, 16.52, 19.54, 23.12 \quad Hz\}$$

The 3-accelerometer channels were processed by the classical spectral estimators: *BTM*, *WPM*, and *MTM* with the channel results and median estimates shown in the figure. Physically, some of the modes were *not* strongly excited at a given accelerometer location and therefore may not appear in the corresponding channel spectrum. This implies that a multichannel processor would provide superior performance in this case, since weak modes over

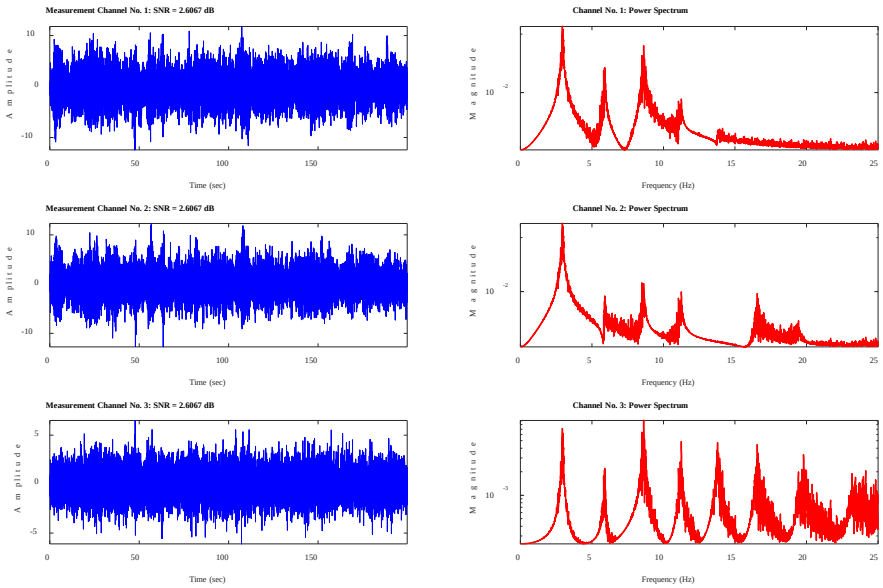

Figure 3: Structural vibrations of 8-mode mechanical system: (a) Accelerometer responses of 3-output system. (b) Fourier power spectra of channel responses.

measurement channels accumulate their response and improve the signal levels. In any case the spectral estimates are shown in Fig. 4a-c for each technique. It is clear in (a) that the *BTM* has a much higher variance and the peaks are difficult to extract even though the power is present at the correct modal frequencies. Both the *WPM* and *MTM* (adaptive) estimates are much smoother than *BTM* (as expected), but their peak resolution has been smeared decreasing the resolution. Six (6) of the 8 modal frequency peaks are clearly discernible, with a 7-th ($23.12Hz$) possible and that at $11.19Hz$ *not* observable. These results are expected based on the previous discussion and bias/variance tradeoff metrics.

Next we applied the three *MTM* weighting techniques to the noisy data sets: *unity*, *eigenvalue* and *adaptive* with the results shown in Fig. 5a-c. Here we see that each of the *MTM*-approaches perform almost identically for this data set when observing the median estimates. Individual channel spectral estimates are also very close with slightly more smoothing by the adaptive method at the higher frequencies. More significant changes can be observed by varying the order of the *DPSS*s. This completes the case study, next we investigate the resolution capability of *MTM*.

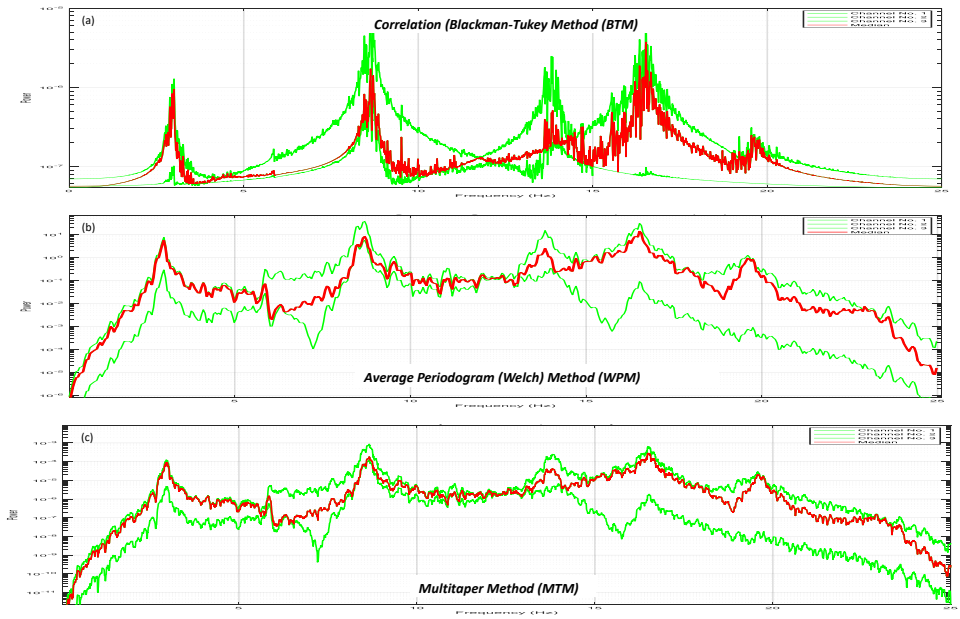

Figure 4: Ensemble Power Spectral Density Estimates for 8-mode, 3-channel structure. (a) Correlation (Blackman-Tukey) method. (b) Welch periodogram method. (c) Multitaper method.

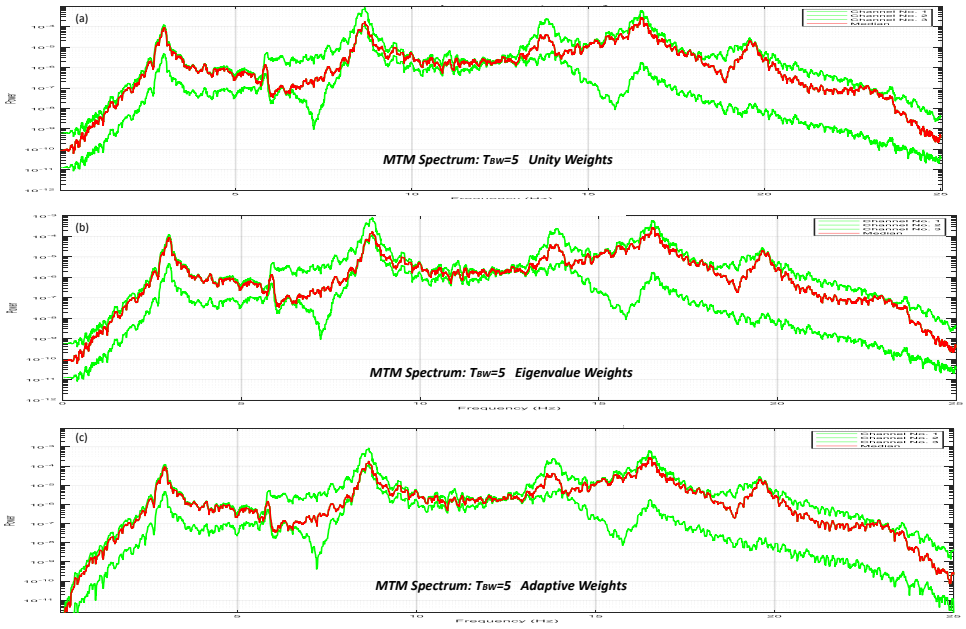

Figure 5: MTM Power Spectral Density Estimates for 8-mode, 3-channel structure. (a) MTM estimates: $T_{BW} = 5$; UNITY weights. (b) MTM estimates: $T_{BW} = 5$; EIGENVALUE weights. (c) MTM estimates: $T_{BW} = 5$; ADAPTIVE weights.

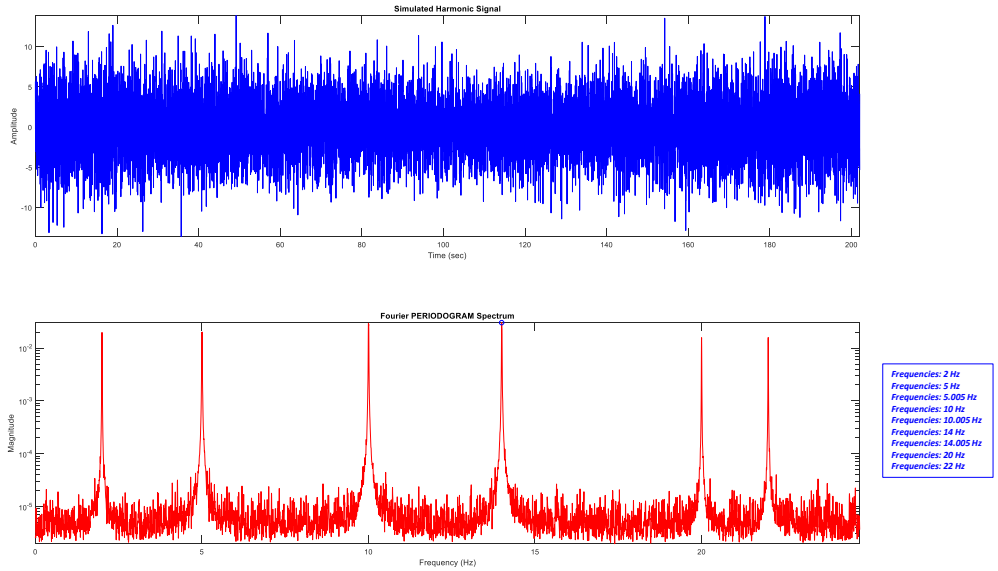

Figure 6: Simulated Sinusoids in Noise (SNR: $-3dB$). (a) Time series. (b) Raw Fourier spectra (FFT).

5 TEST CASE: RESOLUTION OF SINUSOIDS IN NOISE

In this section we synthesize a set of sinusoids in a noisy environment to evaluate the resolution capability of the *MTM*. We developed the algorithms (available in MATLAB) for sinusoidal frequencies at: $\{2, 5, 5\pm0.005, 10, 10\pm0.005, 14, 14\pm0.005, 20, 22Hz\}$ at an signal-to-noise ratio (SNR)[6] of -3 dB SNR.

The synthesized sinusoidal signal is shown in Fig. 6 where we see the noisy time series and its corresponding Fourier spectrum. Next we applied the classical spectral methods and observe the results in the subsequent figure. In Fig. 7a we see the results of the *BTM* and its ability to extract the primary frequencies as well as one of the embedded spectral lines at 5 Hz. The *WPM* results are in (b) where just the primary frequencies are extracted—this is expected since the resolution ability is limited by the limited number of sections and 50% window (Blackman) overlap. The results of the *MTM* are shown in Fig. 7c where we observe its ability to extract all of the sinusoids as well as resolve the close proximity spectral lines at: $5.005Hz, 10.005Hz, and 14.005Hz$ demonstrating its capability. Here we applied the *adaptive-MTM*.

This completes the section, next we summarize the results of this study.

[6]The SNR=signal energy/noise energy: $SNR(dB) = 20log_{10}SNR$.

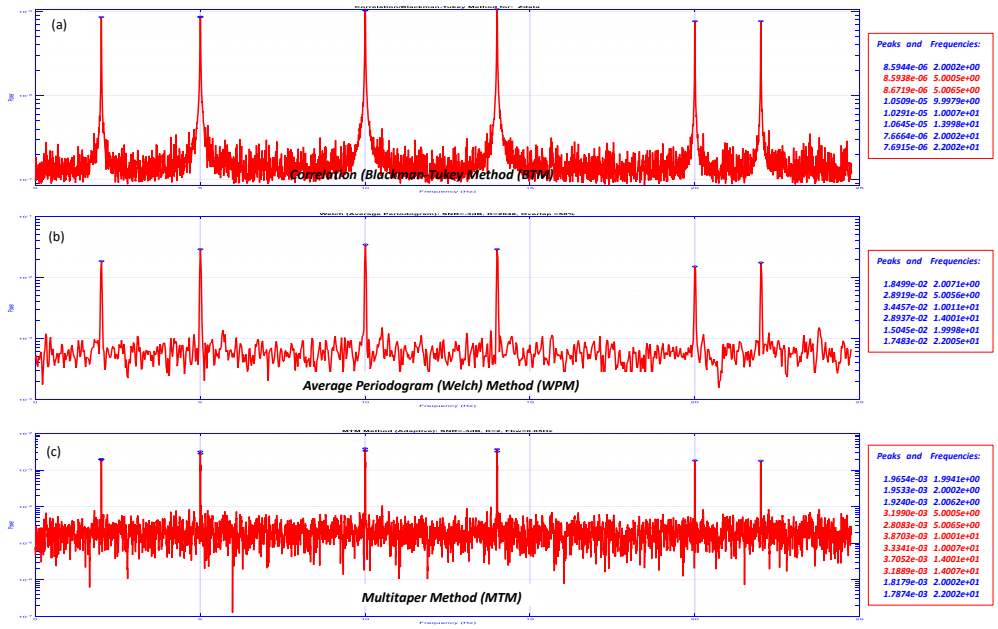

Figure 7: Power Spectral Density Estimates for Sinusoids in Noise (SNR: $-3dB$). (a) Correlation (Blackman-Tukey) method. (b) Welch periodogram method. (c) Multitaper method.

6 SUMMARY

In this report we have investigated the performance of "classical" spectral estimation techniques for single input/single output channel data. We chose the two most popular and well-known techniques: Blackman-Tukey method (BTM) and Welch Periodogram (average) method (WPM). We introduced the lesser known Multitaper method (MTM) and analyzed its properties and performance.

After providing the necessary background material each of these spectral techniques were discussed with the primary emphasis on the MTM. Multiple tapering (windowing) enables a direct solution to the so-called *concentration problem* of providing a set of "optimal" windows that maximize the energy is a certain design bandwidth. From this solution evolves a set of orthonormal *discrete prolate spheroidal sequences* ($DPSS$) or equivalently *Slepian sequences* that can be used to determine the: (1) *number* of $DPSS$-windows required (order estimation); and (2) bias/variance *tradeoff*. The performance metrics and properties of the MTM approach were developed and examined.

A test case evolving from a synthesized 8-mode structural system was developed and investigated to demonstrate the performance of each method indicating there various advantages/disadvantages. However, it became clear that both WPM and MTM techniques were superior to BTM (already known a-priori), but showed the potential advantages of the MTM approach. Resolution issues were not discussed in detail, but it is also known that MTM

is superior to both alternative methods in this regard [11]—an important aspect in modal frequency estimation.

7 Acknowledgments

This work performed under the auspices of the U.S. Department of Energy by Lawrence Livermore National Laboratory under Contract DE-AC52-07NA27344.

References

[1] P. Welch, "The use of fast Fourier transforms for the estimation of power spectra: A method based on time averaging over short modified periodograms," *IEEE Trans. Audio Electroacoust.*, AU-15, 1967.

[2] J. Candy, S. Franco, E. Ruggiero, M. Emmons, I. Lopez and L. Stoops, "Anomaly detection for a vibrating structure: A subspace identification/tracking approach, *J. Acoust. Soc. Am.*, Vol. 142, (2), pp. 680-696, 2017.

[3] M. Junger and D. Feit, *Sound: Structures and Their Interaction*. $2^{Ed.}$ Cambridge, MA: MIT Press, , 1986.

[4] M. R. Hatch, *Vibration Simulation Using MATLAB and ANSYS*. Boca Raton,FL.:Chapman and Hall/CRC Press, 2001.

[5] W. K. Gawronski, *Advanced Structural Dynamics and Active Control of Structures*. London, U.K.:Springer, 2004.

[6] C. Rainieri and G. Fabbrocino, *Operational Modal Analysis of Civil Engineering Structures*. London,U.K.:Springer, 2014.

[7] L. Merovitch, *Analytic Methods in Vibrations*. New York: MacMillan Pubs, 1996.

[8] J. Cooley and J. Tukey, "An algorithm for machine calculation of complex Fourier series," *Math. Comput.*, 1965.

[9] S. Kay, *Modern Spectral Estimation: Theory and Applications*, Englewood Cliffs, New Jersey:Prentice-Hall, 1988.

[10] D. Thomson, "Spectrum estimation and harmonic analysis," *Proc. IEEE*, Vol. 70, No. 9,1982.

[11] D. Percival and A. Walden, *Spectral Analysis for Physical Applications*. $3^{Ed.}$ Cambridge, UK: Cambridge Univ. Press, 1993.

[12] D. Slepian and H. Pollak, "Prolate spheroidal wave functions, Fourier analysis and uncertainty. *Bell Syst. Tech. J.*, Vol. 40., 1961.

[13] J. Candy, *Signal Processing: The Modern Approach* (New York:McGraw-Hill, 1988).

[14] A. Papoulis, *Probability, Random Variables and Stochastic Processes*, New York:McGraw-Hill, 1965.

[15] A. Jazwinski, *Stochastic Processes and Filtering Theory*, New York:Academic Press, 1970.

[16] P. Stoica and R. Moses *Introduction to Spectral Estimation*, Englewood Cliffs, New Jersey:Prentice-Hall, 1997.

[17] J. Markel and A. Gray, *Linear Prediction of Speech*, New York:Springer-Verlag, 1976.

[18] D. Childers, Ed., *Modern Spectral Analysis*, New York:IEEE Press, 1978.

[19] S. Kay and L. Marple, "Spectrum analysis – a modern perspective," *Proc. IEEE*, Vol. 69, 1981.

[20] A. Schuster, "On the Investigation of Hidden Periodicities with Application to a Supposed 26 Day Period of Meteorological Phenomena," *Terrestrial Magnetism*, Vol. 3, 1898.

[21] T. Bronez, "On the performance advantage of multitaper spectral analysis," *IEEE Trans. Sig. Proc.*, Vol. 40, 1992.

[22] A. Walden, "Multitaper estimation of the innovation variance of a stationary time series," *IEEE Trans. Sig. Proc.*, Vol. 43, No. 1, 1995.

[23] S. Haykin, D. Thomson and J. Reed, "Spectrum sensing for cognitive radio," *Proc. IEEE*, Vol. 97, No. 5, 2009.

[24] B. Babadi and E. Brown, "A review of multitaper spectral analysis," *IEEE Trans. Bio. Engr.*, Vol. 61, No. 5, 2014.

[25] J. Candy, *Model-Based Signal Processing*, Hoboken, New Jersey: John Wiley/IEEE Press, 2006.

[26] F. Cara, J. Juan, E. Alarco, E. Reynders, G. De Roeck, "Modal contribution and statespace order selection in operational modal analysis," *Mech. Sys. Sig. Process.*, Vol. 38, 2013.